Open Access

*International journal of Chemistry, Mathematics and Physics (IJCMP)*
*[Vol-4, Issue-6, Nov-Dec, 2020]*
*https://dx.doi.org/10.22161/ijcmp.4.6.1*
*ISSN: 2456-866X*

# Adsorption Isotherms, Kinetics and Thermodynamic Studies of the removal of Manganese from Aqueous Solutions using Activated Carbon Produced from *Lantana camara* stem

Olayiwola Akeem Olusegun*, Kazeem Nimotalai Olabisi

Department of Pure and Applied Chemistry, Analytical/Environmental Chemistry Unit, Ladoke Akintola University of Technology, Ogbomoso, Nigeria.
*Corresponding author: olayiwolaakeem@yahoo.com

Received: 30 Sept 2020; Received in revised form: 06 Nov 2020; Accepted: 11 Nov 2020; Available online: 10 Dec 2020


***Abstract*—** *This study investigated the equilibrium adsorption mechanism and thermodynamics of Manganese (II) ion ($Mn^{+2}$) present in wastewater onto the activated carbon produced from Lantana camara stem as a low cost adsorbent. The Lantana camara stem was carbonized at 300 ˚C for 2 h, ground and chemical-activated. The Chemical-Activated Lantana camara (CALC) stem carbon was characterized using Scanning Electron Microscope (SEM) and Fourier Transform Infrared (FTIR) Spectrophotometry before and after adsorption of $Mn^{2+}$. Batch experiments were conducted at different temperature (35 - 65 ˚C) to study the effects of pH, contact time, adsorbent dosage, initial concentration and temperature of Manganese ion.*

*The FTIR bands at 3425, 2366, 1635, 1446, 1288, and 1116 $cm^{-1}$ were shifted to 3903, 3331, 2378, 2339, 2090, 1845, 1398 and 1342 $cm^{-1}$ after $Mn^{2+}$ adsorption. Similarly, the Scanning Electron Microscopy (SEM) analysis indicated that the average pore size on the activated carbon was 50 µm this shows that $H_3PO_4$ was effective in creating well-developed pores on the surface morphology of the precursor. The Manganese (II) ion ($Mn^{+2}$) uptake increased with increase in pH from 2 to 6. However the uptake of Manganese (II) ion decreased slightly from pH of 8 to 12. The adsorption of Manganese (II) ion having the maximum percentage removal at pH 6. Similarly, there was an increase in the uptake of $Mn^{2+}$ as the dosage increases from 0.5 to 1.0 $g{\cdot}L^{-1}$ and shows slight decreased from 1.5 to 2.5 $g{\cdot}L^{-1}$, at different metal ion concentrations (50 – 200 $mg{\cdot}L^{-1}$) The percentage removal decreased with increasing initial $Mn^{2+}$ concentration for CALC. The $Mn^{2+}$ adsorption increased as contact time increased, and reached equilibrium at 120 minutes. The adsorption capacity decreases more as temperature of the reaction medium increases from 35 to 65 °C, which indicates the exothermic adsorption process of $Mn^{2+}$ onto CALC. The equilibrium adsorption data were analyzed using different model equations such as Langmuir, Freundlich, Temkin and Dubinin- Radushkevich (D-R) isotherms. The experimental results were reasonably correlated by Langmuir ($R^2$ = 0.9915) than other three isotherm models. The maximum adsorption capacity ($q_m$), intensity of adsorption (b) and separation factor ($R_L$) were calculated from Langmuir plot and activation energy of adsorption ($E_a$) was determined from D-R isotherm. The adsorption kinetic data were analyzed using pseudo-*

International journal of Chemistry, Mathematics and Physics (IJCMP)
[Vol-4, Issue-6, Nov-Dec, 2020]
https://dx.doi.org/10.22161/ijcmp.4.6.1
ISSN: 2456-866X

*first-order, pseudo-second-order, intraparticle diffusion and Elovich models. It was found that the pseudo-second order kinetic model was the most appropriate model, describing the adsorption kinetics model ($R^2$ = 0.99). Thermodynamic parameters such as changes in the free energy of adsorption ($\Delta G^o$), enthalpy ($\Delta H^o$) and entropy ($\Delta S^o$) were calculated. The negative values of $\Delta G^o$ indicate that the Manganese (II) ion adsorption process is spontaneous in nature and the negative value of $\Delta H^o$ shows the exothermic nature of the process. The adsorption capacity was evaluated as 147.65 mg/g at 35 °C showing that Lantana camara stem is a promising adsorbent and can be used effectively for the adsorption of metal ions in wastewater.*

***Keywords*— Adsorption, Lantana camara, Manganese, Chemical Activation, Thermodynamic.**

## I. INTRODUCTION

The Naturally occurring Manganese (II) ($Mn^{+2}$) is commonly found in drinking water sources and is essential for human health at low concentrations. On the other hand, excessive ingestion of $Mn^{+2}$ can result in respiratory, reproductive, and especially neurological adverse effects for human beings [1]. According to World Health Organization (WHO), a $Mn^{+2}$ concentrations of 0.05 mg/L in drinking water are usually acceptable to consumers. The permissible limit of $Mn^{+2}$ in drinking water as set by the World Health Organization (WHO) is 0.4 mg/l [2]. Pollution due to the presence of heavy metal ions in water and wastewaters has been a major cause of concern for environmental engineers. There are numerous metals which are significantly toxic to human beings and ecological environments; they include Chromium, Copper, Lead, Cadmium, Mercury, Zinc, Manganese, Nickel, [3]. Heavy metals constitute an important part of environmental pollutants and source of poisoning [4]. Heavy metals are toxic to humans and they persist in the environment. The need for processes to remove heavy metals has received increasing attention [5, 6, 7].

The presence of heavy metal ions is a major concern due to their toxicity to many life forms such as humans, aquatic animals and other living organisms in the environment. Heavy metal contamination exists in aqueous wastes of many industries, such as metal plating, mining operations, tanneries, chloralkali, radiator manufacturing, smelting, alloy industries and storage batteries industries, etc. [8]. Treatment processes for heavy metal removal from wastewater include precipitation, membrane filtration, ion exchange, adsorption, and co-precipitation/ adsorption. Studies on the treatment of effluent bearing heavy metal have revealed adsorption to be a highly effective technique for the removal of heavy metal from waste stream and activated carbon has been widely used as an adsorbent [9].

Several researchers have reported the potential use of agricultural by-products as good adsorbents for the removal of metal ions from aqueous solutions and wastewaters. This process attempts to put into use the principle of using waste to treat waste and become even more efficient because these agricultural by- products are readily available and often pose waste disposal problems. Hence, since they are waste products, they are more cost- effective when compared with the conventional adsorbents like activated carbon. Also, the use of agricultural by-products for wastewater treatment does not involve complicated regeneration process [10]. Many attempts to convert carbonaceous materials into activated carbon for heavy metals removal have been reported in the literature [11]. These include, coconut shell [12], rubber wood sawdust [13], Shells of palm tree [14], Chrysophyllum albidum seed shell [15] Cocoa pod husk Cocoa Pod [16], *Lantana camara* stem [17],Cocoa pod husk [18], *Lantana camara* stem [19] etc. The aim of this present work is to investigate the use of *Lantana camara* stem as an adsorbent for removing heavy metals from aqueous solutions.

## II. MATERIALS AND METHODS

### 2.1 Preparation of chemical activated carbon from *Lantana camara* stems (CALC)

The fresh *Lantana camara* stem used in this research were obtained locally, from the premises of Obada farmer's market at Ipapo area of Oke-Ogun in Oyo State, Nigeria. The stems were separated from the leaves, seeds and flower. The stem were cut into a small pieces and washed with tap water and distilled water to remove sand, debris and other impurities. The sample then sundried for 48 hours until constant weight. It was carbonized at 300 ˚C for 2 h, ground with mortar and pestle and sieved to 2 mm mesh size. The *Lantana camara* stem powder were activated using Phosphoric acid ($H_3PO_4$) for the synthesis of activated carbon from *Lantana camara*

International journal of Chemistry, Mathematics and Physics (IJCMP)
[Vol-4, Issue-6, Nov-Dec, 2020]
https://dx.doi.org/10.22161/ijcmp.4.6.1
ISSN: 2456-866X

stem (CALC) in order to improve the surface properties of the raw powder. The activated carbon sample were then soaked overnight in 1% sodium bicarbonate solution, washed with 0.1M NaOH followed by distilled water repeatedly to remove residual minerals and acid until reached pH 7 after which it oven dry at 110 °C for 24 h and kept in desiccators until further use [20].

### 2.2 Preparation of the Adsorbate

All the chemicals used in this study were of analytical grade and were used without further purification. The adsorbate was prepared by weighing 1 g of $MnCl_4$ powder and dissolving it in small quantity of distilled water in 1000 mL capacity volumetric flask. Distilled water was then added to make up to the mark of the 1000 mL volumetric flask and then stirred rigorously for 5 min to ensure homogeneity and this makes the stock solution (1000 mg/L). Varying concentrations (50 - 200 mg/L) of the stock solution were prepared by serial dilution. The pH of Manganese (II) ($Mn^{+2}$) solutions was adjusted with 0.1 M NaOH or HCl using Equation (1). The initial concentrations of the metal ions were determined using atomic adsorption spectrophotometer AAS (FS-244AA).

$$C_1V_1 \equiv C_2V_2 \quad (1)$$

where $C_1$ is the initial dye concentration; $C_2$ is the final dye concentration; $V_1$ is the initial volume of solution sand $V_2$ is the final volume of solution [21]

### 2.3 Batch Adsorption Experiments

1.0 g of the adsorbent (CALC) was equilibrated with 100 mL of the Manganese (II) ($Mn^{+2}$) solution of known concentration (50 - 200 mg/L) in stoppered borosil glass flask at a different temperature (35 - 65 °C) in an orbital shaker at a constant speed of 145 rpm for 30-120 min. After equilibrium, 30 mL sample was collected from each flask in time intervals of (30, 45, 60 and 120 min); the suspension of the adsorbent was separated from the solution by filtration using centrifugation (EUTECH Instrument) at 2000 rpm for 5 minutes. The concentration of Manganese (II) ion ($Mn^{+2}$) in the solution was measured by atomic absorption spectrophotometer (FS-244AA). The temperature of the solution was maintained at 35°C. The metal ion concentration was measured until the equilibrium was reached. The removal efficiency (% of adsorption or rate of adsorption) of the Manganese (II) ion ($Mn^{+2}$) was calculated using the equation below:

$$\text{Removal efficiency} = \left[\frac{C_0 - C_e}{C_0}\right] \times 100 \quad (2)$$

where $C_0$ (mg/L) is the initial metal ion concentration, $C_e$ (mg/L) is the metal ion concentration at equilibrium.

### 2.4. Batch adsorption studies

The procedures of kinetic experiments were basically identical to those of equilibrium tests. The aqueous samples were taken at preset time intervals, and the concentrations of $Mn^{2+}$ were similarly measured. The amount of adsorption at time t, $q_t$ (mg $g^{-1)}$ was calculated using eqn 3

$$q_t = \left[\frac{C_0 - C_t}{W}\right] V \quad (3)$$

where $C_0$ and $C_t$ (mg $l^{-1}$) are the liquid-phase concentrations of dye at initial and any time t , respectively. V is the volume of the solution and W is the mass of dry adsorbent (g).

## III. ADSORPTION ISOTHERMS

The adsorption isotherm indicates how the adsorption molecules distribute between the liquid and solid phases when the adsorption process reaches an equilibrium state. The analysis of equilibrium adsorption data, by fitting them to different isotherm models. Moreover, analysis of adsorption Isotherm is an important step in environmental pollution control, the key step is to develop an equation which will accurately represent the result and which can be used for design purposes, [22, 23]. Adsorption isotherm in this study was carried out on four well-known isotherms, such as Langmuir, Freundlich, Temkin, and Dubinin-Radushkevich (D-R). The applicability of the isotherm equation was compared by judging the correlation coefficients, ($R^2$).

### 3.1.1 Langmuir Adsorption Isotherm (Model)

The Langmuir equation is valid for monolayer adsorption onto a completely homogenous surface with a finite number of identical sites and with the negligible interaction between adsorbed molecules. The linearised form of Langmuir adsorption model. The Langmuir adsorption isotherm model is successfully used to explain the metal ions adsorbed from the aqueous solutions [24]. The expression of the Langmuir model is given by equation.

$$q_e = \frac{bQ_oC_e}{1+bC_e} \quad (4)$$

Rearranging equation 4, to give equations 5 and 6, makes the equation linearized,

$$\frac{1}{q_e} = \frac{1+bC_e}{bQ_oC_e} \quad (5)$$

$$\frac{1}{q_e} = \frac{1}{Q_o} + \frac{1}{bQ_o} \times \frac{1}{C_e} \quad (6)$$

International journal of Chemistry, Mathematics and Physics (IJCMP)
[Vol-4, Issue-6, Nov-Dec, 2020]
https://dx.doi.org/10.22161/ijcmp.4.6.1
ISSN: 2456-866X

Equation (6) could also be rewritten as expressed in equation

$$\frac{C_e}{q_e} = \frac{1}{bQ_o} + \frac{C_e}{Q_o} \quad (7)$$

Where, $Q_o$ (mg/g) and b (L/mg) are Langmuir constants. $q_e$ is the amount of solute removed or adsorbed at equilibrium (mg/g). $C_e$ is equilibrium concentration of the mixture (mg/L).The values of $Q_o$ and b can be determined respectively from the slope and intercept of the plot of $\frac{C_e}{q_e}$ versus $C_e$ [25].

It has been well documented that the essential characteristics of the Langmuir Isotherm may be expressed in terms of the dimensionless equilibrium parameter,$R_L$, [26,27] also known as the separation factor, given by:

$$R_L = \frac{1}{1+bC_o} \quad (8)$$

$R_L$ has been defined as the isotherm shape that predicts if an adsorption system is favourable or unfavourable. $R_L$ is considered a reliable indicator of the adsorption process. [28, 29]

, stated that $R_L$, indicates the isotherm shape according to the following assumption characteristics: $R_L$, >1 (is unfavorable adsorption); $R_L$= 1 (is linear adsorption); 0< $R_L$, <1 (is favorable adsorption) while $R_L$, = 0 (is irreversible adsorption process).

### 3.1.2 Freundlich Adsorption Isotherm Mode)

The Freundlich Isotherm is an empirical relationship which often gives a more satisfactory model of experimental data [30]. This isotherm is derived from the assumption that the adsorption sites are distributed exponentially with respect to the heat of adsorbed and given by Freundlich [31]. The Freundlich isotherm is an empirical equation employed to describe heterogenous systems. The Freundlich equation is expressed as:

$$q_e = K_F C_e 1/\mathrm{n} \quad (9)$$

Where, $K_F$ is the measure of adsorption capacity and n is the adsorption intensity.

However, the Linearized form of Freundlich equation can be expressed in the form;

$$\log q_e = \log K_F + \frac{1}{n} \log C_e \quad (10)$$

$C_e$ and $q_e$ are equilibrium concentration and adsorption capacity at equilibrium stage. While $K_F$ and n are Freundlich constants which incorporate all factors affecting the adsorption process (adsorption capacity and intensity). Values of $K_F$ and n can be obtained from the intercept and slope of a plot of adsorption capacity, $q_e$ against equilibrium concentration, $C_e$. Both parameters $K_F$ and n affect the adsorption Isotherm. The larger the values $K_F$ and n, the higher the adsorption capacity. Also, the magnitude of the exponent n gives an indication of the favourability of the adsorption process. When the value of n is between 2 and 10 it indicates good adsorption value [32].

**3.1.3 Dubinin–Radushkevich (D-R)** isotherm model was also investigated to evaluate the mean energy of adsorption. It is represented in the linear form by the equation [33].

$$\ln q = ln q_m - \beta_{£^2} \quad (11)$$

$$£ = RTln\left(1 + \frac{1}{C_e}\right) \quad (12)$$

where q is amount adsorbed per gram of the adsorbent (mg/g), $q_m$ is equilibrium adsorption capacity (mg/g) using model, β is Polanyi potential, ε is activity coefficient, $C_e$ is concentration of metal ion in solution at equilibrium(mg/L), R is universal gas constant (8.314J/K/mol) and T is temperature in Kelvin. The values of β and $q_m$ are evaluated from the slope and intercept of the graph of $\ln q$ versus $£^2$ (figs 11-3). The mean energy of adsorption E (kJ $mol^{-1}$) is calculated from the relation [34]:

$$E = \frac{1}{\sqrt{2\beta}} \quad (13)$$

### 3.1.4 Temkin adsorption isotherm

Temkin adsorption isotherm contains a factor that is explicitly entered into the adsorbent adsorbate interactions and characterized by a uniform distribution of the binding energy since it assumes that the heat of adsorption of all molecules in the layer decreases linearly with the coverage owning to adsorbent-adsorbate interactions [35]. The fitting was carried out by plotting the quantity adsorbed $q_e$ against $\ln C_e$. The constants were determined from the slope and the intercept.

The Temkin adsorption isotherm equation is given as:

$$q_e = \left(\frac{RT}{bT}\right) lnKT \ln C_e + \left(\frac{RT}{bT}\right) \quad (14)$$

Where:

$\frac{1}{b_T}$ = adsorption potential of the adsorbent (KJ $mol^{-1}$), KT = Temkin isotherm constant ($dm^3g^{-1}$), $RT$ = Temkin isotherm equilibrium binding constant ($L.g^{-1}$), $bT$ = Temkin isotherm constant

$R$ = Universal gas constant (8.314 $J.mol^{-1}.K^{-1}$), $T$ = Temperature at 298 K., $B$ = Constant related to heat of

International journal of Chemistry, Mathematics and Physics (IJCMP)
[Vol-4, Issue-6, Nov-Dec, 2020]
https://dx.doi.org/10.22161/ijcmp.4.6.1
ISSN: 2456-866X

sorption (J.mol$^{-1}$), *Ce* = adsorbate equilibrium concentration (mg.L$^{-1}$)

### 3.2 Adsorption Kinetics

The study of the kinetics of adsorption is desirable as it provides information about the mechanism and characteristics of adsorption, which is important for efficiency of the process [36]. Adsorption kinetic modeling is very useful for better understanding of Manganese (II) adsorption mechanisms onto *Lantana camara* such as the importance of the chemical reactions and the intra-particle diffusion processes. The kinetics of $Mn^{2+}$ adsorption onto CALC was investigated using four different models: pseudo-first-order kinetic, pseudo-second-order, Elovich Equation and Intra-particle diffusion equation kinetic models were tested at different concentrations in this study to determine which model is in good agreement with experimental $q_e$ (adsorption capacity) value, thus suggesting which model the adsorption system.

### 3.3. Thermodynamic Studies

The Gibbs free energy (ΔG°), the entropy (ΔS°) and the enthalpy (ΔH°) were estimated to determine the feasibility and nature of adsorption process. For determination of ΔH° and ΔS°, the relationship between adsorption equilibrium constant b and Gibbs free energy was calculated at all temperature: using eqns (20) and (21)

$$lnb = \frac{\Delta H^\circ}{RT} + \frac{\Delta S^\circ}{R} \quad (20)$$

The plot of $lnb$ as a function of $\frac{1}{T}$ should give a linear relationship with slope of $\frac{\Delta H^\circ}{R}$ and an intercept of $\frac{\Delta S^\circ}{R}$. Then ΔG° is obtained at any temperature from the following equation:

$$\Delta G^\circ = \Delta H^\circ - T\Delta S^\circ \quad (21)$$

## IV. RESULTS AND DISCUSSION

### 4.1 Characterization of CALC

#### 4.1.1 Fourier Transform Infrared (FTIR) analysis

The FTIR spectra give information about the characteristic functional groups on the surface of the sample before and after the adsorption of $Mn^{2+}$ to ascertain the possible involvement of the functional groups on the surface of CALC in the adsorption of $Mn^{2+}$ presented in Figure. 1a and 1b. The FTIR band at 3425 cm$^{-1}$ can be attributed to O–H stretching of alcohol or carboxylic group, and that at 2366 cm$^{-1}$ can be assigned to C–H stretching of an aliphatic of methyl group. A sharp absorption band at 1635 cm$^{-1}$ is assigned to N-H bending vibration of carbonyl compound, bands at 1446-1288 cm$^{-1}$ can be attributed to C-O stretching vibration of carboxylic acid and a broad absorption at 1116 cm$^{-1}$ is assigned to C–O bending vibration of an alcohol. A sharp prominent absorption band at 3903 cm$^{-1}$ was due to C=O stretching vibration of carboxylic acid. In the CALC spectrum, after the adsorption some of the functional groups were shifted to higher wave number 3903 cm$^{-1}$ C=O stretching vibration of carboxylic acid, 3331 cm$^{-1}$ O–H stretching of alkane, 2378-2339 cm$^{-1}$ of C≡N stretching vibrations of alkynes, 2090 cm$^{-1}$ assigned to the C≡C stretching vibrations of an alkyne, 1845 cm$^{-1}$ may be attributed to C=O stretching vibrations of aldehydes/ketone and 1398-1342 cm$^{-1}$ N-O symmetric stretching of aromatic of nitro compounds. There are indication that the absorption bands identified in the spectra and corresponding functional groups in the adsorbent could enhance the surfaces on which adsorption would take place. The changes in spectra confirm the effect of the acid activation resulting in a reduction, broadening, disappearance or appearance of new peaks after acid activation of CALC.

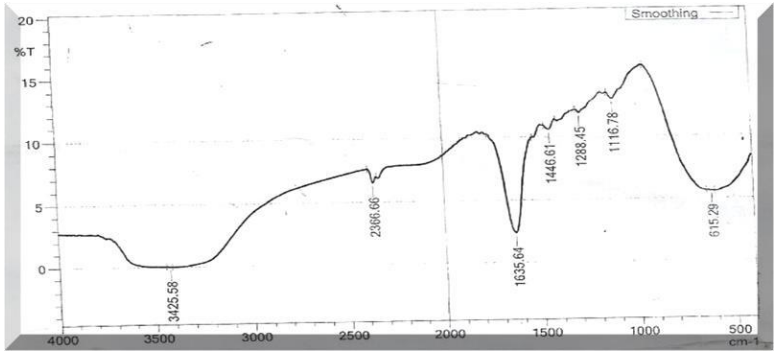


*Fig.1a. FTIR of spectrum CALC before adsorption*

International journal of Chemistry, Mathematics and Physics (IJCMP)
[Vol-4, Issue-6, Nov-Dec, 2020]
https://dx.doi.org/10.22161/ijcmp.4.6.1
ISSN: 2456-866X

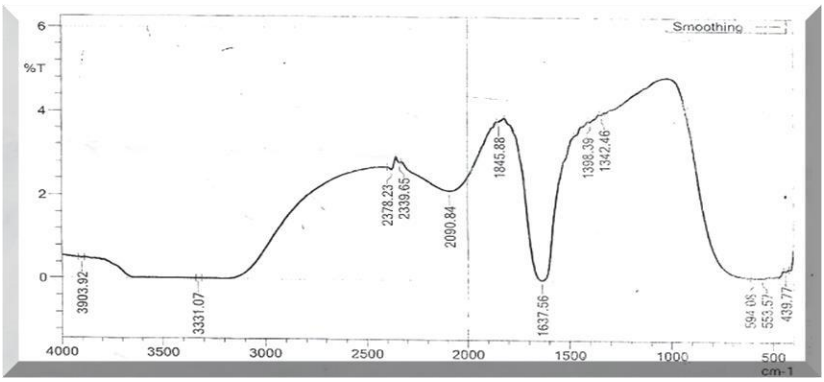


*Fig.1b. FTIR of spectrum CALC after adsorption*

**4.1.2 Scanning Electron Micrograph (SEM) of Chemical Activated *Lantana camara* (CALC) is shown in Plate 1(a) and (b), respectively.**

Plate 1a and 1b: shows the scanning electron micrograph (SEM) of *Lantana camara* Activated Carbon before (a) and after (b) adsorption of Manganese (II) ion. There was a significantly microscopic morphology change in both plates.

. From the plate 1a, it is clear that CALC surface was rough, uneven and the pores were not properly developed in shape, whereas, in Plate 1(b), there are several pores formed on the CALC. This shows that $H_3PO_4$ was effective in creating well-developed pores on the surface morphology of the precursor, thus, leading to activated carbon with large surface area and porous surface structure. These pores provided a good surface for $Mn^{2+}$ to be trapped and adsorbed [20, 30].

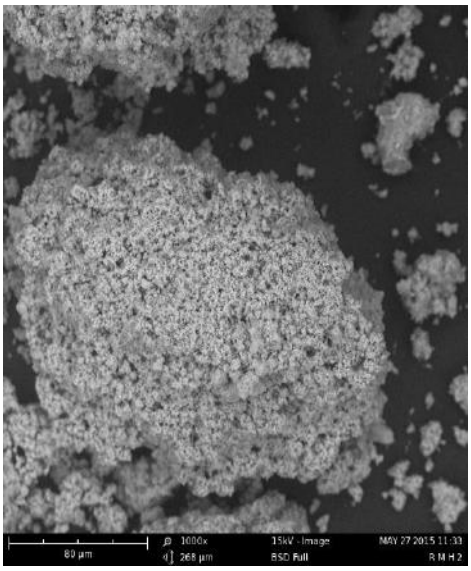


*(a)*

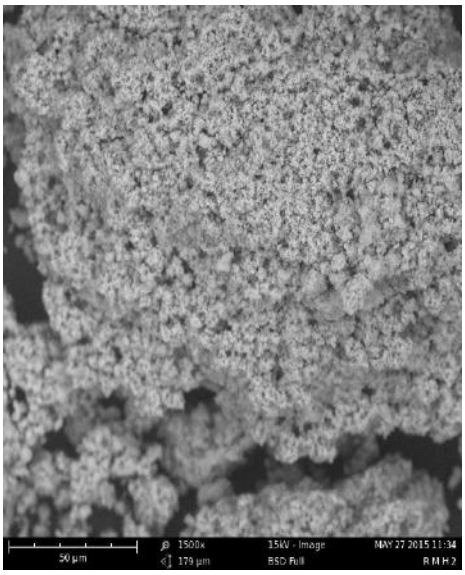


*(b)*

*Plates: 1. Scanning electron microscope of (a) fresh CALC and (b) $Mn^{2+}$ adsorbed CALC*

***4.2 Effect of pH on Adsorption* of $Mn^{2+}$ onto ACLC**

The pH of the aqueous solution is an important controlling parameter in the adsorption process.

It was observed that the pH was affected by the amount of Manganese (II) ion as shown in fig.2. The percentage removal for the adsorption of Manganese (II) ion increased with increase in pH from 2 to 6. However the uptake of Manganese (II) ion decreased slightly from pH of 8 to 12. The adsorption of Manganese (II) ion having the maximum percentage

International journal of Chemistry, Mathematics and Physics (IJCMP)
[Vol-4, Issue-6, Nov-Dec, 2020]
https://dx.doi.org/10.22161/ijcmp.4.6.1
ISSN: 2456-866X

removal at pH 6. The minimum percentage removal observed at low pH was due to large amount of hydroxonium ion ($H_3O^+$) which competed with the positively charged metal ions ($Mn^{2+}$) for the adsorbent surface sites, therefore, the available surface area and subsequent adsorption of the metal ion was reduced. The increase in metal ion removal as pH increases could be explained on the basis of a decrease in competition between hydroxonium ions and metal species for the surface sites and also by the decrease in positive surface charge on the adsorbents, which resulted in a lower electrostatic repulsion between the surface and the metal ions. and hence uptake of metal ions increased. A similar report was proposed by several earlier workers for metal adsorption on different adsorbents [20, 37].

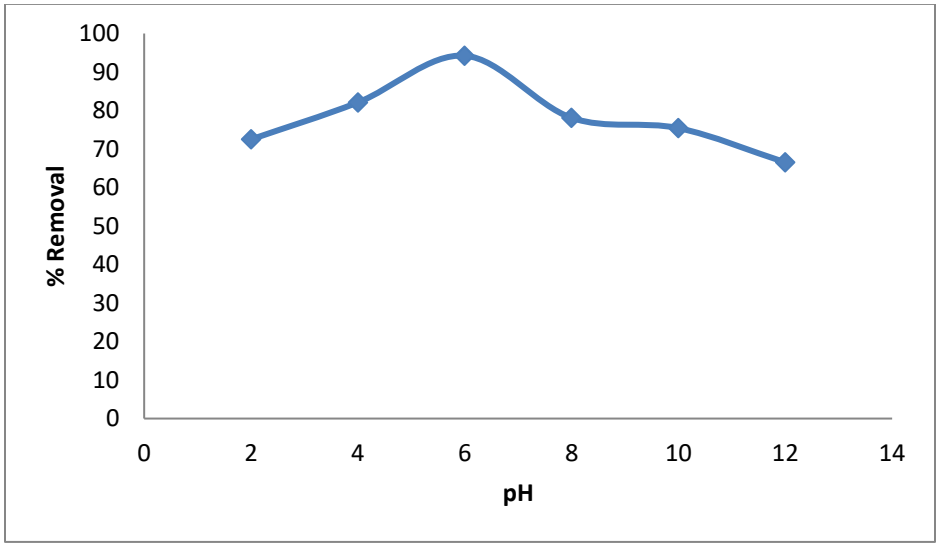


*Fig.2: Effect of pH on adsorption of $Mn^{2+}$ onto ACLC*

### 4.3. Effect of adsorbent dosage on *Adsorption* of $Mn^{2+}$ onto CALC

Fig. 3 shows that the limited number of the adsorbing species is present for a relatively larger number of available surface sites on the adsorbent at higher dosages. This support the fact that at higher dosages of the adsorbent there would be higher availability of exchangeable sites from metals ions uptake [29]. The highest adsorption was observed when the dose was increased from 0.5 to 1.0 g. further addition of the adsorbent beyond 1g dose uptake; this is probably due to overlapping of adsorption sites a consequence of overcrowding of adsorbent particles. The optimum removal of $Mn^{2+}$ (88.80%) was obtained in the adsorbent dose of 1.0 g.

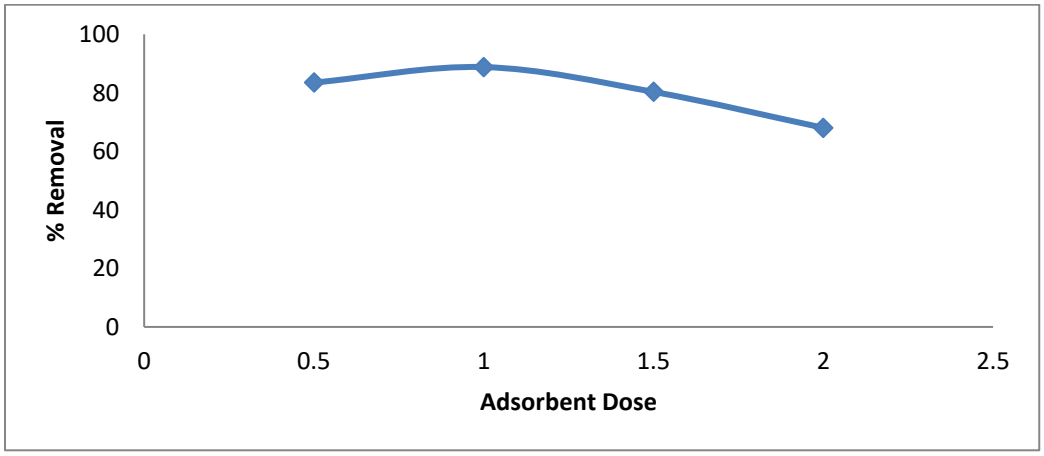


*Fig.3: Effect of adsorbent dosage on Adsorption of $Mn^{2+}$ onto CALC*

*International journal of Chemistry, Mathematics and Physics (IJCMP)*
*[Vol-4, Issue-6, Nov-Dec, 2020]*
*https://dx.doi.org/10.22161/ijcmp.4.6.1*
*ISSN: 2456-866X*

### 4.4 Effect of Initial Concentrations *on Adsorption* of $Mn^{2+}$ onto CALC

The effect of initial concentration of the metal ions on the adsorption rate of $Mn^{2+}$ from the aqueous solution was studied for the metal ion concentrations ranging from 50 - 200 ppm.

Figure 4. Shows the effect of initial concentrations of $Mn^{2+}$ on % removal by CALC. The % removal decreased with increasing initial $Mn^{2+}$ concentrations. The lower uptake at higher concentration resulted from an increased ratio of initial adsorption number of moles of the metal ions to the available surface area; hence fractionally becomes dependent on initial concentration. The initial metal ions concentration provides an important driving force to overcome the mass transfer resistance of the metal ions between the aqueous and solid phases. Therefore, at higher initial metal ions concentration, the number of ions competing for the available sites on the surface of CALC was high, resulting in higher $Mn^{2+}$ adsorption capacity [38]. Similar results were reported by [28]. With 1.0 g of adsorbent at pH 4 the maximum adsorption is obtained for concentrations 50 - 100 ppm.

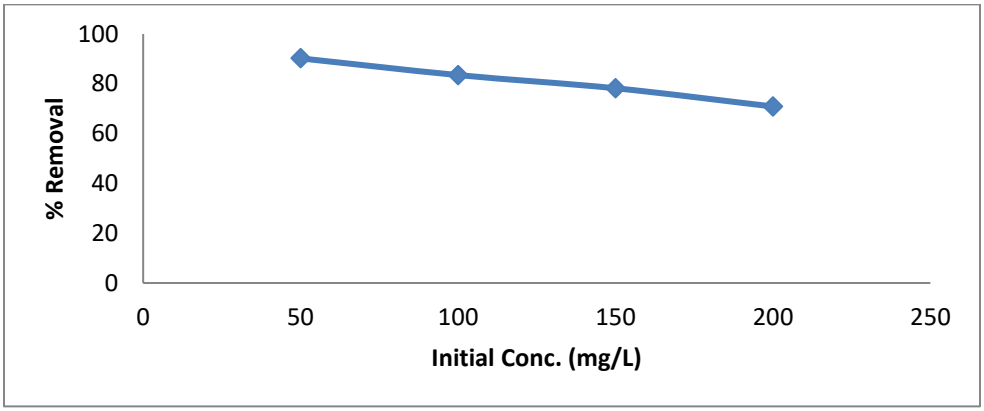


*Fig.4: Effect of Initial Concentrations on Adsorption of $Mn^{2+}$ onto CALC*

### 4.5. Effect of contact time on *adsorption* of $Mn^{2+}$ onto CALC

The contact time is one the effective factor in batch adsorption process and it is necessary to determine the contact time to reach equilibrium. The $Mn^{2+}$ adsorption uptake was increased as contact time increased from 35-120 mins and reaches equilibrium at 120 minutes (**Figure .5**). The result suggests that, adsorption takes place rapidly at the initial stage on the external surface of the adsorbent followed by a slower internal diffusion process, which may be the rate determining step [20, 39]. In addition, the fast adsorption at the initial stage may be due to the fact that a large number of surface sites are available for adsorption but with time, the remaining surface sites are difficult to be occupied. This is because of the repulsion between the solute molecules of the solid and bulk phases, thus, taking longer time to reach equilibrium [40].

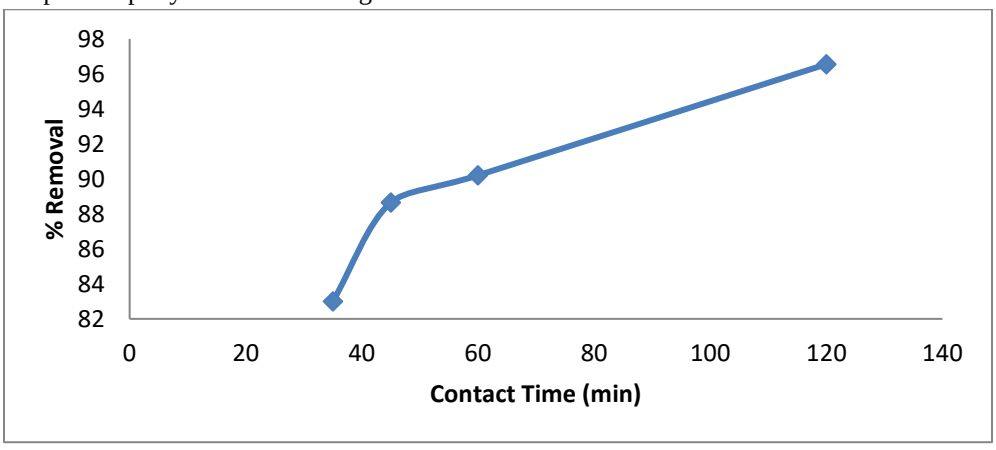


*Fig.5: Effect of Contact Time on Adsorption of $Mn^{2+}$ onto CALC***4**

*International journal of Chemistry, Mathematics and Physics (IJCMP)*
*[Vol-4, Issue-6, Nov-Dec, 2020]*
*https://dx.doi.org/10.22161/ijcmp.4.6.1*
*ISSN: 2456-866X*

**.6 Effect of temperature on *adsorption* of $Mn^{2+}$ onto CALC**

Temperature is an important parameter that influence metal ions adsorption. The various adsorption tests were carried out at different temperatures ranging from 35 °C to 65 °C, using 100 $mgl^{-1}$ initial $Mn^{2+}$ concentrations at pH 6 and with a dose of 1.0 g of activated carbon. As shown in Fig. 6. It was observed that the adsorption capacity decreases more as temperature of the reaction medium increases from 35 °C to 65 °C, which indicate the exothermic adsorption process of $Mn^{2+}$ onto CALC. The amount of $Mn^{2+}$ adsorbed was 96.55% at 35 $^0$C, 90.20% at 45 °C, 88.65% at 55 $^0$C and 83.00 at 65 $^0$C. According to [41]; this phenomenon could be explained by the adsorption of Manganese (II) ions caused by an increase in the thermal energy available. Increasing the temperature would induce greater mobility of the adsorbate, leading to the adsorption of Manganese (II) ions [42].

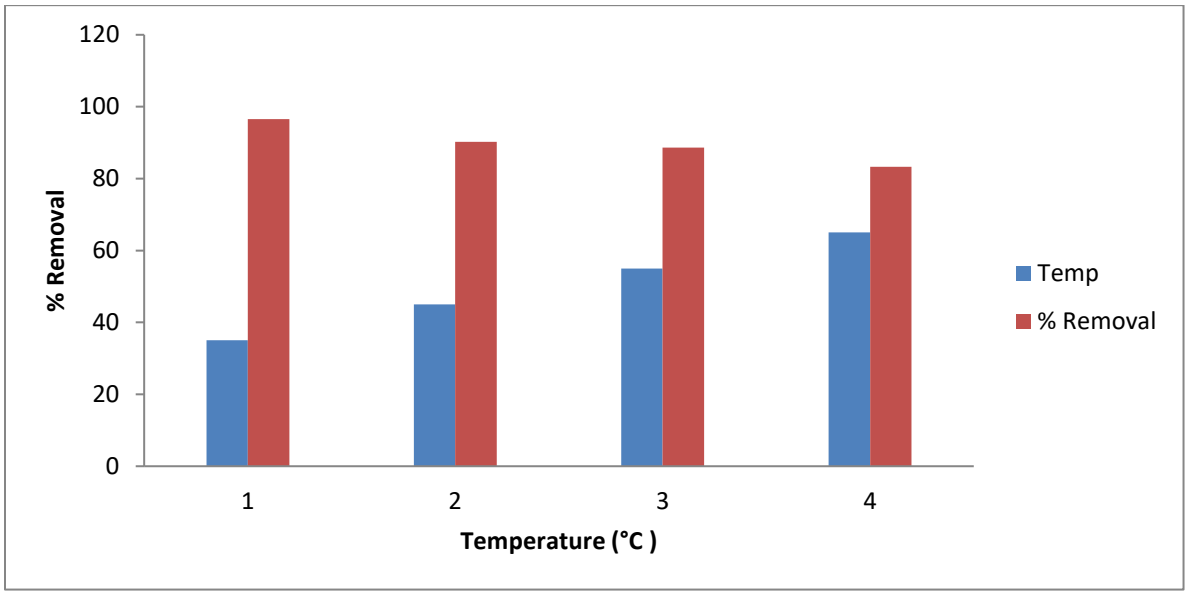


*Fig.6: Effect of temperature on the adsorption of Manganese (II) ions onto CALC*

Figure 7 shows the linear plot of the ratio of equilibrium concentration to mass of the adsorbent versus equilibrium concentration. The plot has $R^2$ value of 0.9915 with a slope and intercept values of 0.1939 and 2.2865 respectively. The values of the Langmuir constants (b, $Q_0$and$R_L$) for the adsorption of Mn (II) ion onto CALC were determined from the slope and intercept values and are shown in Tables 1.

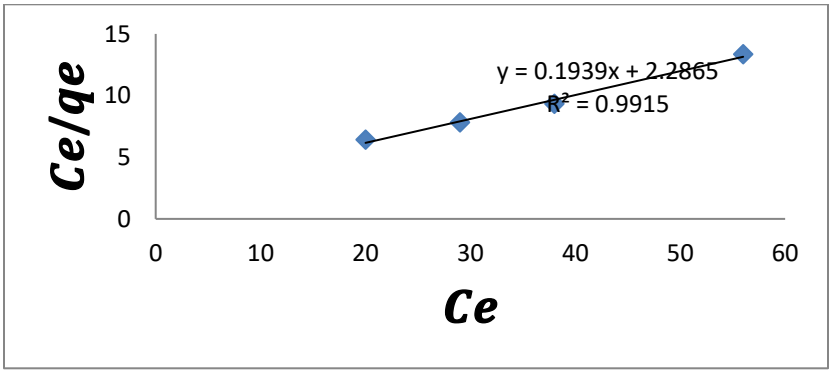


*Fig.7: Langmuir Isotherm for Adsorption of $Mn^{2+}$ onto CALC*

*International journal of Chemistry, Mathematics and Physics (IJCMP)*
*[Vol-4, Issue-6, Nov-Dec, 2020]*
*https://dx.doi.org/10.22161/ijcmp.4.6.1*
*ISSN: 2456-866X*

Figure: 8: shows linear plot of log $q_e$ versus log $C_e$ with a Correlation Coefficient ($R^2$) value of 0.9084. The slope and intercept are 0.1382 and 0.4494 respectively. The Freundlich parameters ($K_F$and n) for the adsorption of Mn (II) ion onto CALC were determined from the slope and intercept as tabulated in Table 1.

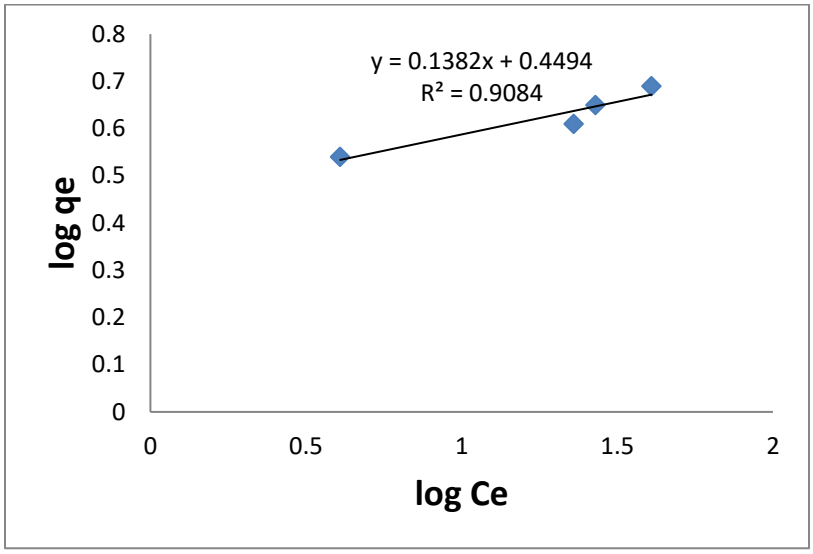


*Fig.8: Freundlich Isotherm for Adsorption of $Mn^{2+}$ onto CALC*

Figure 9, shows the linear form of the Dubinin- Radushkevich isotherm plot of ln $q_e$ versus **£²** with a Correlation Coefficient ($R^2$) of 0.9578, with slope and intercept of 0.024 and 0.3431 respectively. The Dubinin- Radushkevich parameters ($q_D$and B) that are related to mean free energy of adsorption per mole of the adsorbate ($mol^2/J^2$) were determined from the slope and intercept values tabulated in Table 1.

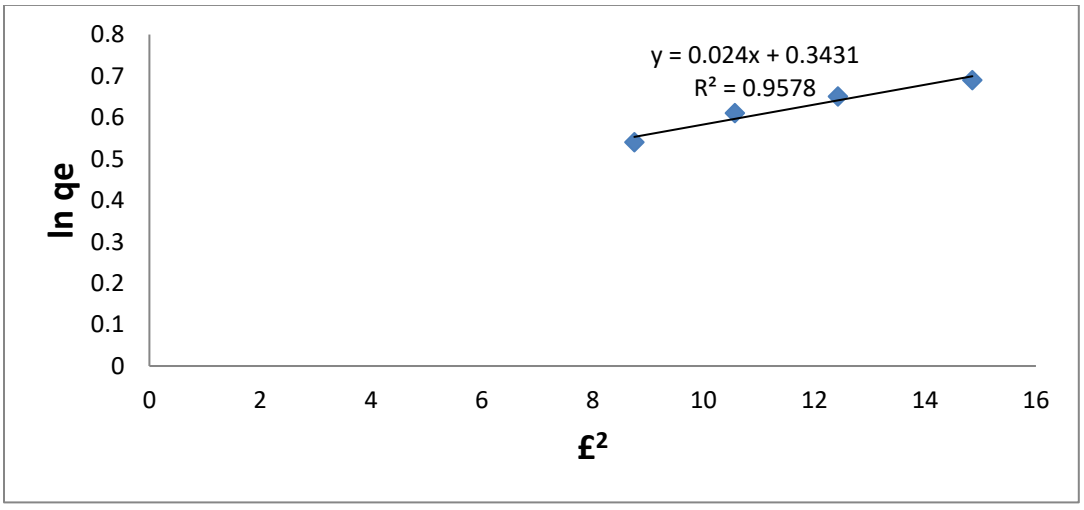


*Fig.9: Dubinin-Radushkevich Isotherm for Adsorption of $Mn^{2+}$ onto CALC*

Figure 10 shows plot of the Temkin isotherm energy constant. The slope and intercept obtained from the graphical plot of $q_e$ against ln $C_e$ with a Correlation Coefficient ($R^2$) of 0.9227, slope and intercept of 0.9594 and 0.4246 respectively. The Temkin parameters ($K_T$ and $b_T$) are related to mean free energy of adsorption are determined from the slope and intercept values as tabulated in Table 1.

International journal of Chemistry, Mathematics and Physics (IJCMP)
[Vol-4, Issue-6, Nov-Dec, 2020]
https://dx.doi.org/10.22161/ijcmp.4.6.1
ISSN: 2456-866X

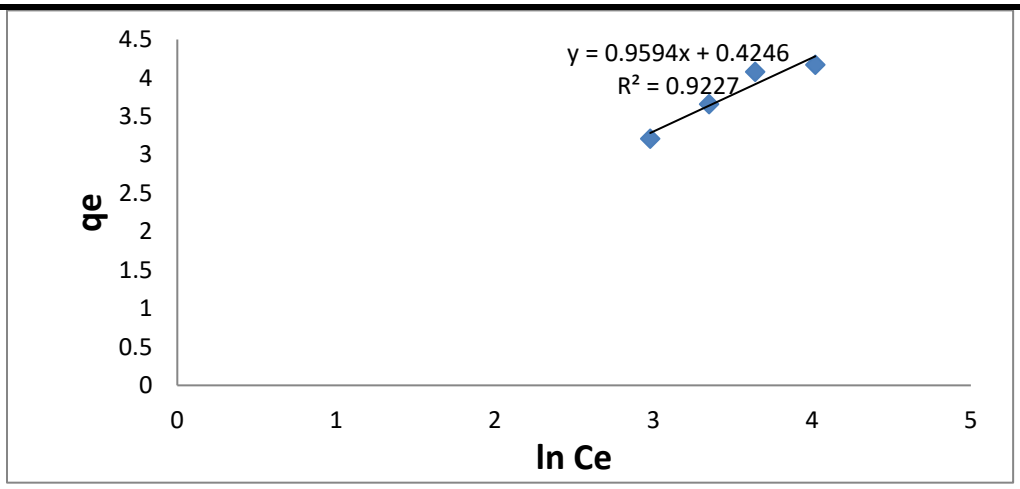


*Fig.10: Temkin Isotherm for Adsorption of $Mn^{2+}$ onto CALC.*

As presented in Table 1, the adsorption capacity was evaluated as 147.65 mg/g at 35 °C, the high $R^2$ values were obtained from all isotherms, whereas the highest value belongs to Langmuir isotherm with 0.9915. This indicates occurrence of homogeneous and monolayer adsorption coverage on the used adsorbent. $\frac{1}{n}$ Value, calculated in accordance with Freundlich equation, indicates whether the adsorption process is spontaneous. Spontaneous adsorption conditions indicate where *n* values are greater than 1 [43]. In the present study *n* value was found to be lesser than 1. Accordingly, it can be inferred that CALC is applicable for removal of $Mn^{2+}$ from aqueous solutions. Also, the activation energy (*Ea*), resulting from Dubinin-Radushkevich equation, was found as 13.984, which indicates that the adsorption occurred with ion exchange since this value falls within 8-16 kJ/mol interval. $R^2$ was found as 0.9578 for Temkin isotherm, indicating that adsorption also conforms to Temkin model. *b* value was found as 0.098 g.J/mg.mol. This low *b* value is an indication of exothermic adsorption [44].

*Table 1: List of Isotherm model statistical parameters for the adsorption of Manganese (II) onto CALC at different temperatures.*

| | Temperatures (°C) | | | |
|---|---|---|---|---|
| Isotherm Model | 35 | 45 | 55 | 65 |
| Langmuir | | | | |
| $q_m$ (mg/g) | 147.65 | 133.35 | 112.93 | 105.87 |
| b (L/mg) | 0.098 | 0.086 | 0.078 | 0.073 |
| $R_L$ (g/mg) | 0.963 | 0.915 | 0.848 | 0.784 |
| $R^2$ | 0.9915 | 0.9903 | 0.9746 | 0.9683 |
| Freundlich | | | | |
| $K_F$ (L/g) | 1.69 | 1.53 | 1.33 | 1.25 |
| 1/n | 0.852 | 0.785 | 0.734 | 0.586 |
| $R^2$ | 0.9084 | 0.9053 | 0.9033 | 0.9015 |
| Dubinin- Radushkevich | | | | |
| $q_e$ (mg/g) | 27.432 | 24.631 | 21.841 | 19.860 |
| $\beta$ ($mol^2/KJ^2$) | 4.523 | 3.869 | 3.568 | 2.856 |

International journal of Chemistry, Mathematics and Physics (IJCMP)
[Vol-4, Issue-6, Nov-Dec, 2020]
https://dx.doi.org/10.22161/ijcmp.4.6.1
ISSN: 2456-866X

| | | | | |
|---|---|---|---|---|
| $E_a$(kJ/ mol) | 13.984 | 11.464 | 9.461 | 7.915 |
| $R^2$ | 0.9578 | 0.9504 | 0.9462 | 0.9326 |
| Temkin | | | | |
| $K_T$ (L/g) | 0.586 | 0.332 | 0.237 | 0.197 |
| $b_T$ (J/mol) | 0.674 | 0.643 | 0.585 | 0.546 |
| $R^2$ | 0.9227 | 0.9027 | 0.9206 | 0.9069 |

**Effect of temperature and adsorption thermodynamics**

The optimum temperature for manganese (II) ion adsorption of CALC was 35 °C and fall within the temperature range studied. Thermodynamic parameters Gibbs free energy change, ($\Delta G^o$) was calculated using Langmuir constants (Table 2). The enthalpy change, ($\Delta H^o$) and the entropy change,( $\Delta S^o$), for the adsorption process were calculated to give the values −3.13 and 11.23 J/mol K, respectively. The negative values of ΔG° confirm the feasibility of the process and the spontaneous nature of adsorption due to high preference for $Mn^{2+}$ onto CALC. The value of ($\Delta H^o$) is negative, indicating that the adsorption reaction is exothermic. The positive value of (ΔS°) reflects the affinity of the CALC for $Mn^{2+}$ and suggests some structural changes in $Mn^{2+}$ and CALC interaction [34]. The thermodynamics parameters ΔG°, $\Delta H^o$ and ΔS° of different temperature was tabulated in table 2.

*Table.2: Thermodynamic parameters for the adsorption of $Mn^{2+}$ onto CALC at different temperatures.*

| Temperatures (°C) | $\Delta G^o$ (kJ/mol) | $\Delta H^o$ (kJ/mol) | $\Delta S^o$ (kJ/mol K) |
|---|---|---|---|
| 35 | -586 | | 11.23 |
| 45 | -6.05 | -3.13 | |
| 55 | -6.16 | | |
| 65 | -6.23 | | |

The Pseudo-first-order-model can be expressed [45]; [46]; [47]; [48].

$$log\ (q_e - q_t) = log q_e - \frac{k_1 t}{2.303} \qquad (16)$$

Where,$q_e$, $q_t$ (mg/g) are the mass of the metal ion adsorbed at equilibrium (adsorptive capacity), and mass adsorbed at any time‘t’, $k_1$, ($min^{-1}$) is the equilibrium constant of the pseudo-first-order adsorption. The value of $k_1$ and $q_e$ are determined respectively from the slope and intercept of the plot of $log\ (q_e - q_t)$ versus t.

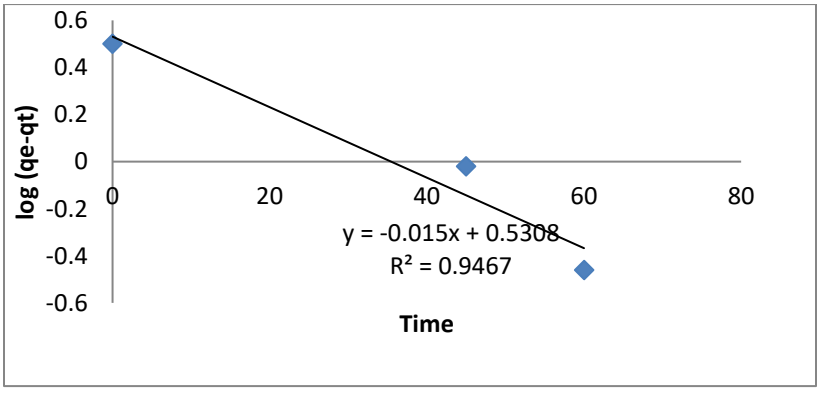


*Fig. 11. Pseudo first order kinetic for adsorption of $Mn^{2+}$ onto CALC.*

*International journal of Chemistry, Mathematics and Physics (IJCMP)*
*[Vol-4, Issue-6, Nov-Dec, 2020]*
*https://dx.doi.org/10.22161/ijcmp.4.6.1*
*ISSN: 2456-866X*

The corresponding pseudo-second-order model is expressed thus [34];

$$\frac{1}{q_t} = \frac{1}{k_2 q_{e2}} + \frac{1}{q_e} \times t \qquad (17)$$

Where, $k_2$ ($gmg^{-1}min^{-1}$), t, and $q_e$, are the Pseudo-second-order rate constant, time, and adsorption capacity at equilibrium respectively. The value of $q_e$ is determined from the plot of $\frac{t}{q_t}$ versus t.

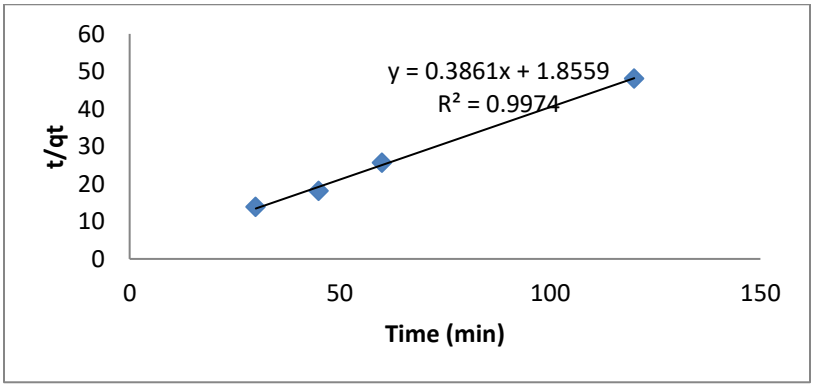


*Fig. 12: Pseudo second order kinetic for adsorption of $Mn^{2+}$ onto CALC.*

The intraparticle diffusion equation can be written as follows [49]:

$$q_t = k_{dif}\, t^{0.5} + C \qquad (18)$$

where $q_t$ is the amount of the adsorbate adsorbed at time t, C is the intercept, and $k_{dif}$ is the intraparticle diffusion rate constant (mg $g^{-1}$ $min^{-1}$). The kinetic results were tested by the intraparticle model to elucidate the diffusion mechanism. The values of $q_t$ correlated linearly with the values of $t^{0.5}$ (Shown in Figure: 13), and the rate constant $k_{dif}$ was directly evaluated from the slope of the regression line. The intercept of the plot reflects the boundary layer effect. The larger the intercept, the greater the contribution of the surface adsorption in the rate controlling step. The calculated intraparticle diffusion coefficient $k_{dif}$ values are listed in Table **3.** If the regression of $q_t$ vs. $t^{0.5}$ is linear and passes through the origin, then intraparticle diffusion is the sole rate-limiting step. [49].

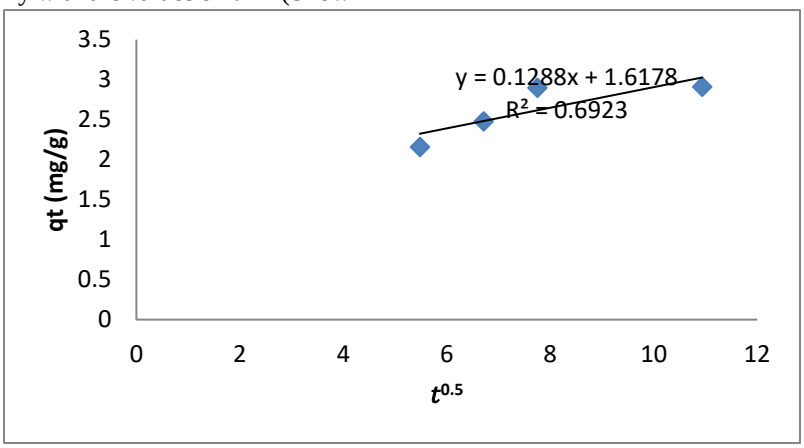


*Fig. 13: Intrapartcle diffusion kinetic for adsorption of $Mn^{2+}$ onto CALC.*

***The Elovich model***

The Elovich equation is suitable in describing the kinetics of adsorption on heterogeneous solids. The Elovich model equation is generally expressed by Equation (19): [50] $q_e = \left(\frac{1}{\beta}\right)\ln(a\beta) + \left(\frac{1}{\beta}\right)\ln t \qquad (19)$

*International journal of Chemistry, Mathematics and Physics (IJCMP)*
*[Vol-4, Issue-6, Nov-Dec, 2020]*
*https://dx.doi.org/10.22161/ijcmp.4.6.1*
*ISSN: 2456-866X*

where α is the initial adsorption rate (mg/g.min) and β is the adsorption constant of surface coverage and activation energy for chemisorption (g/mg) during any experiment. The slope and intercept of the plot of $q_e$ vs. ln $t$ can be used to calculate the values of the constants $\alpha$ and $\beta$, respectively. There was increased in initial adsorption rate $\alpha$ and decreased in desorption constant $\beta$ with an increase in initial dye concentration. A similar result was reported by [51].

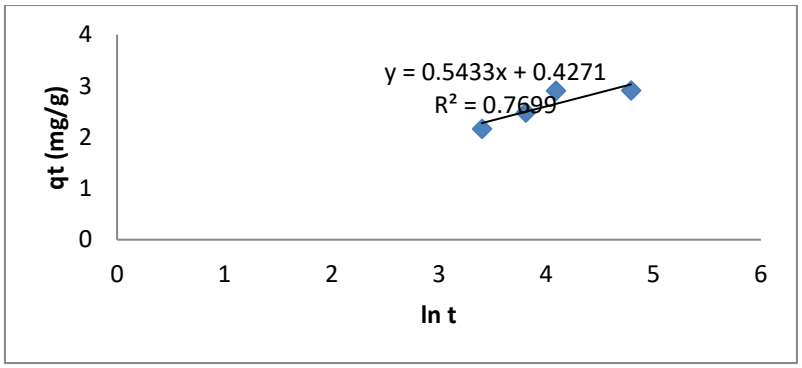


*Fig.14: Elovich kinetic for Adsorption of $Mn^{2+}$ onto CALC.*

The kinetic parameters calculated using four different models pseudo first order, pseudo second order, intra particle diffusion and elovich were tabulated in table 3. From the comparative analysis of all the four tested models, it was observed that the pseudo second order model have the highest **$R^2$ 0.99** for all the concentration and temperature used for the experimental studies the predictions of $q_e$ for all the tested conditions was closed to the experimental value of $q_e$ which show that these was a good agreement between the experimental and predicted values. These indicate that the adsorption system is probably best described by the pseudo-second order kinetic model. Manganese ions were adsorbed on the surface of activated carbon via chemical interaction such as ionic or covalent bonds [52]. Similar phenomena for biosorption of heavy metal ions were reported in previous studies [53, 54, 55]. Kinetic models such as intra-particle diffusion model and Elovich equation demonstrate an important role of the pore diffusion process in the adsorption mechanism. As seen in Figure 13 and 14 respectively the $Mn^{2+}$ adsorption on CALC coincides with the origin for all pH values and it occurs in two steps. The rate constants for two resultant steps were in the order $k_1 < k_2$ , and the *C* values at each step increased with increasing pH. This is an indication of increased in boundary layer thickness with increasing pH, which in turn results in a decrease in the diffusion rate. The first and the second linear sections can be respectively attributed to the external mass transfer and intra particle diffusion mechanisms [51, 53].

*Table 3. List of calculated Parameters for kinetic parameters for Manganese (II) adsorption onto Lantana camara stem at different concentrations and temperatures.*

| Kinetics Model | **Concentrations (mg/L)** | | | | **Temperatures ($^0$C).** | | | |
|---|---|---|---|---|---|---|---|---|
| | **50** | **100** | **150** | **200** | **35** | **45** | **55** | **65** |
| **First order kinetics** | | | | | | | | |
| $K_1 \times 10^{-2}$ (min$^{-1}$) | 0.46 | 0.98 | 0.48 | 0.47 | 0.69 | 0.87 | 0.76 | 0.75 |
| $q_e$ exp (mg g$^{-1}$) | 34.31 | 84.23 | 62.09 | 60.35 | 34.24 | 48.96 | 46.87 | 47.86 |

*International journal of Chemistry, Mathematics and Physics (IJCMP)*
*[Vol-4, Issue-6, Nov-Dec, 2020]*
*https://dx.doi.org/10.22161/ijcmp.4.6.1*
*ISSN: 2456-866X*

| | | | | | | | | |
|---|---|---|---|---|---|---|---|---|
| $q_e$ cal (mg $g^{-1}$) | 28.33 | 63.42 | 60.52 | 60.00 | 34.37 | 48.62 | 46.53 | 46.37 |
| $R^2$ | 0.9463 | 0.9467 | 0.9360 | 0.9348 | 0.9454 | 0.9441 | 0.9356 | 0.9431 |
| SSE (%) | 1.495 | 5.203 | 0.393 | 0.088 | 0.033 | 0.085 | 0.130 | 0.373 |
| **Second order kinetics** | | | | | | | | |
| $K_2 \times 10^{-4}$ (mg $g^{-1}$ $min^{-1}$) | 14.85 | 28.73 | 46.49 | 56.53 | 9.88 | 16.64 | 26.35 | 28.97 |
| $q_e$ cal (mg $g^{-1}$) | 36.39 | 86.57 | 62.95 | 60.55 | 34.38 | 48.86 | 46.54 | 47.55 |
| $R^2$ | 0.9918 | 0.9974 | 0.9954 | 0.9943 | 0.9989 | 0.9968 | 0.9964 | 0.9967 |
| SSE (%) | 0.520 | 0.585 | 0.215 | 0.175 | 0.035 | 0.025 | 0.083 | 0.078 |
| **Intra particle diffusion** | | | | | | | | |
| $k_{dif}$ (mg $g^{-1}$ $min^{-1}$) | 1.894 | 1.946 | 2.893 | 3.889 | 2.425 | 2.843 | 2.432 | 2.332 |
| C | 14.85 | 23.74 | 24.86 | 26.69 | 15.69 | 18.83 | 26.31 | 26.96 |
| $R^2$ | 0.6843 | 0.6923 | 0.6641 | 0.6532 | 0.6975 | 0.6671 | 0.6643 | 0.6471 |
| **Elovich** | | | | | | | | |
| $\alpha$ (mg $g^{-1}$ $min^{-1}$) | 0.549 | 0.837 | 0.454 | 0.432 | 12.092 | 14.371 | 18.653 | 29.892 |
| β (mg $g^{-1}$) | 3.985 | 5.496 | 8.697 | 8.975 | 6.715 | 10.969 | 16.856 | 28.968 |
| $R^2$ | 0.7632 | 0.7699 | 0.6371 | 0.6891 | 0.6796 | 0.6873 | 0.6899 | 0.6874 |

### 4.4. *Test of kinetic models*

Besides the value of $R^2$, the applicability of both pseudo-first order kinetic model and pseudo-second order kinetic model out of the four model used are verified through the sum of error squares (SSE, %). The adsorption kinetics of $Mn^{2+}$ on activated carbon derived from CALC was tested at different initial concentrations. The validity of each model was determined by the sum or error squares (SSE, %) given by:

$$\text{SSE } (\%) = \frac{\sqrt{\Sigma(q_{e\,exp} - q_{ecal})^2}}{N} \quad (22)$$

where $N$ is the number of data points. The higher is the value of $R^2$ and the lower is the value of

SSE; the better will be the goodness of fit. Table 3 lists the calculated results. It is found that the adsorption of manganese (II) ion onto CALC produced from *Lantana camara* stem can be best described by the second-order kinetic model. Similar phenomena processes have been observed in the adsorption of methylene blue on activated carbon prepared from *Chrysophyllum albidum* seed shell [41] and Scavenging Rhodamine B dye using Moringa Oleifra seed pop [44].

## V. CONCLUSION

This present study described the adsorption of manganese (II) onto activated carbon produced from *Lantana camara* stem. The suggested adsorbent showed promising results in removing metal ions from synthetic wastewater under the studied conditions. In batch adsorption studies, data showed that activated *Lantana camara* stem had relatively considerable potential for the removal of manganese (II) ion from aqueous solution. Langmuir isotherm fitted very well with studied temperature and concentration ranges. The $R_L$ values showed that activated *Lantana camara* stem was favorable for the adsorption of manganese (II) ion. The suitability of the kinetic models for the adsorption of manganese (II) onto activated *Lantana camara* stem was also investigated. It was clear that the adsorption kinetics of manganese (II) onto activated *Lantana camara* stem followed

*https://dx.doi.org/10.22161/ijcmp.4.6.1*
*ISSN: 2456-866X*

pseudo-second-order adsorption kinetics. The value of $\Delta H^O$, $\Delta S^0$ and $\Delta G^0$ result shows that the process was exothermic, spontaneous and thermodynamically feasible. Therefore it is recommended that CALC produced from *Lantana camara* stem could be used for remediation of metal ion from wastewater. *Lantana camara* stem are a low cost natural abundant adsorbent material in Nigeria and it may be alternative to more costly adsorbent materials.

## THE COMPLIANCE WITH ETHICAL STATEMENT

Funding: This study was funded by the authors. Has no research grants from any Company.

Conflict of Interest: The authors declare that they have no conflict of interest with this paper.

## REFERENCES

[1] Vinod Pahade and A. K. Sharma "Manganese Removal by Low Cost Adsorbent from Synthetic Wastewater-A Review", International Journal of Engineering Research ISSN: 2319- Volume No.4, Issue No.3, pp: 111 – 114, 2015.

[2] Taffarel Silvio Roberto and Rubio Jorge "On the removal of $Mn^{2+}$ ions by adsorption onto natural and activated Chilean zeolites" Minerals Engineering, vol. 22, pg. 336–343, 2009.

[3] A.K.Meen, K. Kadirvelu, G.K. Mishraa, C. Rajagopal and P. N. Nagar "Adsorption of Pb (II) and Cd (II) metal ions from aqueous solutions by mustard husk". Journal of Hazardous. Materials. 150 619–625, 2008.

[4] F .E. Okeimen, V. U. Onyenkpa "Binding of cadmium, copper, lead and nickel ions with melon (Citrullus vulgaris) seed husk", Biological Waste, vol. 29, 11–16, 2000.

[5] Afkhami A and Moosavi R "Adsorptive removal of Congo red, a carcinogenic textile dye, from aqueous solutions by maghemite nanoparticles". Journal of Hazardous Materials, 174: 398–403, 2010.

[6] Chen YH, Li FA "Kinetics study on removal of $Cu_2$ using goethite and hematite nano photocatalystss". *Journal* of *Colloid* and *Interface Science*, 347, 277–281, 2010.

[7] Ezoddina M, Shemirania F, Abdib Kh, Khosravi Saghezchia M, Jamalic MR "Application of modified nano-alumina as a solid phase extraction sorbent for the preconcentration of Cd and Pb in water and herbal samples prior to flame atomic Absorption spectrometry determination". Journal of *Hazardous* Materials, 178, 900–905, 2010.

[8] Kadirvelu, K., Thamaraiselvi, K, and Namasivayam, C., "Removal of Heavy Metal from Industrial Wastewaters by Adsorption onto Activated Carbon Prepared from an Agricultural Solid Waste". *Bioresource Technology*, **76**, pp. 63-65, 2001.

[9] Chand, S., Aggarwal V.K. and Kumar P., "Removal of Hexavalent Chromium from the Wastewater by Adsorption. *Indian Journal of Environmental Health*, **36** (3): pp. 151-158, 1994.

[10] A. Abia, J. C. Igwe, "Sorption kinetics and intraparticulate diffusivities of Cd, Pb, and Zn ions on Maize Cob", Journal of *Biotechnology*, vol. 4, 509–512, 2005.

[11] J.M. Dias, M.C.M. Alvim-Ferraz, M.F.Almeida, J.Rivera-Utrilla, M.Sánchez-Polo, "Waste materials for activated carbon preparation and its use in aqueous-phase treatment: are view", Journal of *Environmental Management*, vol. 85, 833–846, 2007.

[12] M. Sekar, V.Sakthi, S.Rengaraj, "Kinetics and equilibrium adsorption study of lead (II) onto activated carbon prepared from coconut shell", J. Colloid Interface Sci., 279, pp. 307–313, 2004.

[13] M.H. Kalavathy, T. Karthikeyan, S.Rajgopal, L. R. Miranda "Kinetic and isotherm studies of Cu (II) adsorption onto $H_3PO_4$ activated rubber wood sawdust". *Journal* of *Colloid* and *Interface Science*, 292, 354–362, 2005.

[14] S. Gueu, B. Yao, K.Adouby, G. Ado. "Heavy metal removal in aqueous solution by activated carbon prepared from coconut shell and seeds hell of the palm tree", *Journal of Applied Sciences*. 6, 27–89, 2006.

[15] Amuda O.S., Edewor T.I., Azeez, G.O. and Elesaodo C. B. "Kinetics and equilibrium studies of adsorption of cadmium using steam activated carbon prepared from chrysophyllum albidum seed shell". Journal of Environmental Chemistry and Ecotoxicology, Vol. 3(3), pp. 203-213, 2011.

[16] Bello, O.S., and M.A. Ahmad, "Adsorptive Removal of Synthetic Dye Using Cocoa Pod Husks." *Toxicological and Environmental Chemistry*, 93, (7): 1298–1308, 2012.

[17] Girish and Murty. "Adsorption of Phenol from Aqueous Solution Using Lantana camara, Forest Waste: Packed Bed Studies and Prediction of Break through Curves", *Springer International Publishing Switzerland*, 2, 773–796, 2015.

[18] Moses Olabode Olakunle, Adejunmoke Abosede Inyinbor, Adewumi Oluwasogo Dada and Olugbenga Solomon Bello. "Combating Dye Pollution Using Cocoa Pod Husks: a Sustainable approach", *International Journal of Sustainable Engineering*. 04, 29, pp 01-12 2017. https://doi.org/10.1080/19397038.2017.1393023.

[19] Vipin Kumar Saini, Surindra Suthar, Chaudhari Karmveer, and Kapil Kumar. "Valorization of Toxic Weed *Lantana camara* L. Biomass for Adsorptive Removal of Lead", Hindawi Journal of Chemistry,1-12, 2017. https://doi.org/10.1155/2017/5612594.

[20] Amuda OS, Edewor TI, Afolabi TJ, Hung Y-T. "Steam-activated carbon prepared from Chrysophyllum albidum seed shell for the adsorption of cadmium in wastewater: Kinetics, equilibrium and thermodynamic studies". *International*

*Journal* of *Environment* and *Waste Management*. 12, (2), 213-229, 2013.

[21] Vadivelan, V. and Kumar, K.V., "Equilibrium and Kinetic mechanism and process design for the adsorption of methylene blue onto rice husk". *Journal* of *Colloid* and *Interface Science*, **286,** (1), 90-100, 2005.

[22] Aksu Z. "Determination of equilibrium, kinetic and thermodynamic parameters of the batch biosorption of nickel (II) ions onto *Chlorella vulgaris*. Process". *Journal of Biochemistry* 38, 89-99, 2002.

[23] Langmuir, I. "The adsorption of gases on plane surfaces of glass, mica and platinum". *Journal of the American Chemical Society*, **40,** (9), 1361-1403, 1918.

[24] Langmuir I. "The constitution and fundamental properties of solids and liquids". *Journal of the American Chemical Society*, 38, 2221-2295, 1916.

[25] Hall, K.R., Eagleton, L.C., Acrivos, A. and Vermeulen, T. "Pore-and Solid-Diffusion Kinetics in Fixed-Bed Adsorption under Constant-Pattern Conditions". *Industrial and Engineering Chemistry Fundamentals*, **5**, 212-223, 1966. http://dx.doi.org/10.1021/i160018a011

[26] Bello, O.S., Fatona, T.A., Falaye, F.S., Osuolale, O.M. and Njoku, V.O. "Adsorption of Eosin Dye from Aqueous Solution Using Groundnut Hull-Based Activated Carbon: Kinetic, Equilibrium, and Thermodynamic Studies". *Environmental Engineering Science*, **29**, 186-194, 2011.

[27] Alade, A.O., Amuda, O.S., Afolabi, T.J. and Okoya, A.A. "Adsorption of Naphthalene onto Activated Carbons Derived from Milk Bush Kernel Shell and Flamboyant Pod". *Journal of Environmental Chemistry and Ecotoxicology*, **4**, 124-132, 2012.

[28] Amuda OS, Olayiwola AO, Alade AO, Farombi AG, Adebisi SA. "Adsorption of methylene blue from aqueous solution using steam-activated carbon produced from *Lantana camara* Stem". *Journal of Environmental Protection*, 5, 1352-1363, 2014.

[29] Amuda, O.S., Adelowo, F.E. and Ologunde, M.O. "Kinetics and Equilibrium Studies of Adsorption of Chromium (VI) Ion from Industrial Wastewater Using *Chrysophyllum albidum* (Sapotaceae) Seed Shells". *Colloid Surface B*: *Bio Interface*, **68**, 184-192, 2009.

[30] Bello, O.S., Adeogun, A.I., Ajaelu, C.J. and Fehintola, E.O. "Adsorption of Methylene Blue onto Activated Carbon Derived from Periwinkle Shells: Kinetics and Equilibrium Studies", Colloids *and* Surfaces B*: Bio Interfaces Chemistry and Ecology*, **24**, 285-295, 2008. http://dx.doi.org/10.1080/02757540802238341

[31] Freundlich, H.M.F. "Über die adsorption in lösungen", *Zeitschrift für physikalische Chemie* (*Leipzig*), **57**, 385-470, 1906.

[32] Mckay, G., "Adsorption of dyes on chitin equilibrium studies". *Journal of Applied Polymer Science*, **27**, 3043-3057, 1982.

[33] Igwe, J. C.; Abia, A. A. "Equilibrium sorption isotherm studies of Cd (II) Pb (II) and Zn(II) ions detoxification from waste water using unmodified and EDTA-modified maize husk". *Electronic Journal of Biotechnology*, 10, 536–548, 2007.

[34] Ho, Y. S. and Mckay, G., "A comparison of chemosorption kinetic models applied to pollutant removal on various sorbents", *Pro Safety and Environmental Protection*, 76B, 4, 332-340, 1998.

[35] Davoud Balarak, Ferdos Kord Mostafapour, Hossein Azarpira and Ali Joghataei "Langmuir, Freundlich, Temkin and Dubinin– radushkevich Isotherms Studies of Equilibrium Sorption of Ampicilin unto Montmorillonite Nanoparticles", *Journal of Pharmaceutical Research International, 20, (2), 1-9, 2017.*

[36] Bello, O. S., M. Auta, and O. B. Ayodele. "Ackee Apple (*Blighia sapida*) Seeds: ″A Novel Adsorbent for the Removal of Congo Red Dye from Aqueous Solutions", *Journal of Chemistry and Ecology*, 29, (1), 58–71, 2013.

[37] Girish and Murty. "Adsorption of Phenol from Aqueous Solution Using *Lantana camara*, Forest Waste: Kinetics, Isotherm, and Thermodynamic Studies, *Hindawi Publishing Corporation International Scholarly Research Notices*, 16, 2014. http://dx.doi.org/10.1155/2014/201626.

[38] Patnukao, P; Kongsuwan, A; Pavasant, P. "Batch studies of adsorption of copper and Pb (II) on activated carbon from Eucalyptus camaldulensis Dehn. Bark", *Journal of Environmental Science,* 20, 1028 – 1034, 2008.

[39] Adebayo, GB; Mohammed, AA; Sokoya, SO. "Biosorption of Fe (II) and Cd (II) ions from aqueous solution using a low cost Adsorbent from Orange Peels", *Journal of Applied* Sciences and *Environmental Management*, Vol. 20, (3), 702-714, 2016.

[40] Gialamouidis, D., Mitrakas, M. and Liakopoulou-Kyriakides, M. "Equilibrium, Thermodynamic and Kinetic Studies on Biosorption of Mn (II) from Aqueous Solution by *Pseudomonas* sp., *Staphylococcus xylosus* and *Blakeslea trispora* Cells". *Journal of Hazardous Materials*, **182**, 672-680, 2010. http://dx.doi.org/10.1016/j.jhazmat.2010.06.084

[41] Amuda OS, Adebisi SA, Olayiwola AO, Farombi AG, Adejumo AL. "Adsorption Isotherms and Kinetics studies of the removal of methylene blue from aqueous solutions using *Chrysophyllum albidum* seed shell", *Journal of Applied Chemical Science International*, 6, (2), 63-73, 2016.

[42] Malakootian M, balarak D, Mahdavi Y, Sadeghi SH, Amirmahani N. "Removal of antibiotics from wastewater by azolla filiculoides: Kinetic and equilibrium studies", International Journal on Applications in Pharmaceutical and Biological Sciences, 4, (7), 105 113, 2015.

[43] Hameed B, Mahmoud D, Ahmad A. "Sorption of basic dye from aqueous solution by pomelo (Citrus grandis) peel in a batch system", *Colloids* and *Surfaces A: Physicochemical* and *Engineering Aspects*, 316, (1), 78-84, 2008. DOI: 10.1016/j.colsurfa.

[44] Olugbenga Solomon Bello, Bukola Morenike Lasisi, Olamide Joshua Adigun and Vunain Ephraim "Scavenging Rhodamine B dye using Moringa Oleifra seed pop", *Chemical Speciation & Bioavailability*, 29,1, 120-134 2017.

[45] Lagergren, S. "About the Theory of So-Called Adsorption of Soluble Substance", *Kungliga Svenska Vetenskapsakademiens Handlingar*, **24**, 1-39, 1898.

[46] Ho, Y., and G. McKay. "The Sorption of Lead (II) Ions on Peat", *Water Research*, 33, 578–584, 1999.

[47] Amuda OS, Giwa AA, Bello IA. "Removal of heavy metal from industrial wastewater using modified activated coconut shell carbon", B*iochemistry Engineering Journal*, 36, 174-181, 2007.

[48] Adebisi SA, Amuda OS, Adejumo AL, Olayiwola AO, Farombi AG. "Equilibrium, kinetic and thermodynamics studies of adsorption of aniline blue from aqueous media using steam-activated carbon prepared from *Delonix regia* Pod", *Journal of Water R*esources *Protection*, 7:1221-1233,2015. Available:http://dx.doi.org/10.4236/jwarp.2015 .715099

[49] Aksu Z, Tunc O. "Application of biosorption for *Penicillin G* removal: Comparison with *Balarak* activated carbon". Process Biochemistry. 40, (2), 831-847, 2005.

[50] Zazouli MA, Mahvi AH, Mahdavi Y, Balarakd D. "Isothermic and kinetic modeling of fluoride removal from water by means of the natural biosorbents sorghum and canola. Fluoride", *Journal of Water R*esources *Protection*, 4, 8(1), 15-22, 2015.

[51] Aboua Kouassi Narcissea, Yobouet Yao Augustinb, Soro Donafologo Babaa, Yao kouassi Benjaminb, Meite Ladjia, Diarra Moussaa, Traore Karim Sorya, Trokourey Albert. "Equilibrium, kinetic and thermodynamic studies of chromium adsorption by activated carbon from the shell of tieghmelia heckelii fruit", *International Journal of Engineering Science and Technology* (IJEST), Vol. 9, No.12, 1074- 1082, 2017.

[52] Mekonnen E, Yitbarek M. and Soreta TR "Kinetic and thermodynamic studies of the adsorption of Cr (VI) onto some selected local adsorbents", South African *Journal of Chemistry*, 68, 45–52, 2015

[53] Mohammad Abul Hossain, Md. Lokman Hossain and Tanim-al-Hassan "Equilibrium, Thermodynamic and Mechanism Studies of Malachite Green adsorption on Used Black Tea Leaves from Acidic Solution", *International Letters of Chemistry, Physics and Astronomy, Vol. 64, pp 77-88, 2016.*

[54] Fan T, Liu Y, Feng B, Zeng G, Yang C, Zhou M, "Biosorption of cadmium (II), zinc (II) and lead (II) by Penicillium simplicissimum: Isotherms, kinetics and thermodynamics". J Hazard Mater.160, 655-66, 2008. DOI: 10.1016/j.jhazmat.2008.03.038.

[55] Joo JH, Hassan SHA and Oh SE. "Comparative study of biosorption of $Zn^{2+}$ by Pseudomonas aeruginosa and Bacillus cereus". Int Biodeterioration Biodegrad. 64, 734-74, 2010. DOI: 10.1016/j.ibiod.2010.08.007.